Cross-Plane Acquisitions in Electrical Capacitance Volume Tomography

Rafiul K. Rasel, *Student Member, IEEE*, Joshua N. Sines, Qussai Marashdeh, *Senior Member, IEEE*, and Fernando L. Teixeira, *Fellow, IEEE*

***Abstract*—Electrical capacitance tomography (ECT) is a widely used imaging modality to image two-dimensional cross sections of multiphase flows. Recent developments in electrical capacitance volume tomography (ECVT) have made it possible to directly obtain volumetric images from measured data. ECVT is instrumental for obtaining accurate phase hold up information and velocity information that are needed for optimization of certain flow processes. However, compared to ECT, the high correlation between measurements in ECVT exacerbates the ill-conditioning of the associated image reconstruction problem. Previous studies have suggested that neglecting mutual capacitance data between ECVT electrodes located at cross-planes that are well separated along the sensor axis can be done without significantly affecting the reconstructed image. In addition, this may help constrain the ill-conditioning of the reconstruction problem. In this paper, we examine in detail and quantify the effect of reduced cross-plane acquisition strategies for optimizing image reconstruction and constraining the ill-conditioning of typical ECVT settings.**

***Index Terms*—Electrical capacitance tomography, capacitive sensors, cross-plane measurements, process tomography, real time sensing.**

I. Introduction

MULTIPHASE flows such as gas-solid-liquid reactor systems are very common in industrial processes [1]. The behavior of multiphase flows can vary widely based on the dynamics of various constituent phases. To optimize many complex industrial processes it is highly desirable to have accurate phase hold up information of the multiphase flow [2]–[6]. Two-dimensional electrical capacitance tomography (ECT) is widely used to obtain flow information in the cross-section of a region of interest (RoI) [7]–[15]. However, accurate *volumetric* information is necessary to better understand and optimize multiphase flow processes. Electrical capacitance volume tomography (ECVT) enables to directly obtain volumetric images of the RoI from the measured data [16]–[19]. Volumetric images are also crucial for many other aspects such as flow velocity profiling [20] and volume fraction measurement. The amount of axial information that can be extracted by ECVT sensors mainly depends on the sensor design [12], [21] and the number of sensor cross-planes (layers). Both ECT and ECVT are based on the measurement of mutual capacitances between electrodes positioned at the outer boundary of the RoI, which is typically a cylinder vessel containing the multiphase flow. However, the high degree of correlation (redundancy) between measurements in ECVT exacerbates the ill-conditioned nature of the image reconstruction problem [22]. Another key challenge in ECVT is that the number of possible measurements and the associated acquisition complexity (in terms of the required electronics and overall data acquisition time) increases rapidly with each additional sensor plane. For example, an 8 electrode ECT sensor yields 28 independent mutual capacitance measurements. On the other hand, a ECVT sensor with 10 layers with 8 electrodes on each yields 3160 independent measurements. These challenges increase the hardware deployment costs and can make real-time operation more difficult.

A simple solution to capture a RoI with large volume in ECVT is to increase the axial height of each electrode. Although effective in increasing the sensed volume, this strategy reduces the axial resolution and decreases the sensitivity between electrodes spaced across several layers. As an example, Fig. 1 shows cross-plane measurement results for a 10 layer 8 electrode ECVT sensor. Capacitance measurements are collected for a reference (empty) RoI using three different ECVT sensors with varying electrode heights, $h = 0.15r$, $0.3r$, and $0.9r$, where r is the radius of the cylindrical vessel. All other characteristics are identical among these three ECVT sensors. It is clear from the figure that the cross-plane capacitances, and hence the signal-to-noise ratio (SNR), decreases rapidly with electrode height. It should be noted that due to this low SNR for larger electrode height measurements between any electrode pair separated by 1 sensor layers will not provide valuable information and should be discarded.

A fundamental question thus arises: For a given RoI volume and electrode height, what is the optimal choice of the number of cross-plane measurements to be included? There are very few works that aims at optimizing ECVT measurement acquisitions [23] and reduce the computational cost. Past work on cross-plane measurements is very scarce in the context of interrogating fields that are Laplacian (quasi-static) in nature inside the RoI, such as in the ECVT scenario. Clearly, if no cross-plane measurements are included, available information is missing and the achievable resolution can be affected. On the other hand, if the entire set of cross-plane measurements are included, measurements with very low SNR (across far apart layers) and high correlation will be included in the data set which, as noted before, would increase the ill-conditioning

R. K. Rasel and F. L. Teixeira are with the ElectroScience Laboratory, Department of Electrical and Computer Engineering, The Ohio State University, Columbus, OH 43212 USA (e-mail: rasel.1@osu.edu, teixeira.5@osu.edu).

J. S. Shines and Q. M. Marashdeh are with Tech4Imaging LLC, Columbus, OH 43220 USA (e-mail: marashdeh@tech4imaging.com).

This work was supported by the U.S. Department of Energy under grants Nos. DE-SC0011936 and DE-SC0010228 and by NASA Space Technology Mission Directorate under under grant No. NNX16CC10C.

Manuscript received MM DD, YYYY; revised MM DD, YYYY.

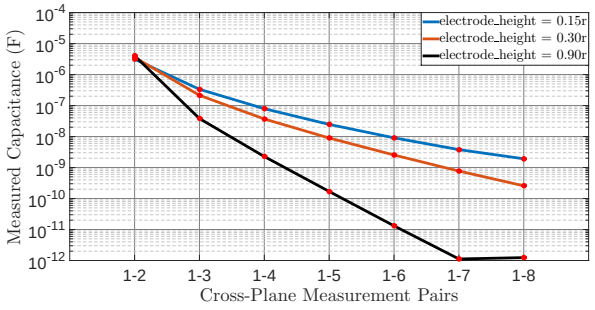

(a)

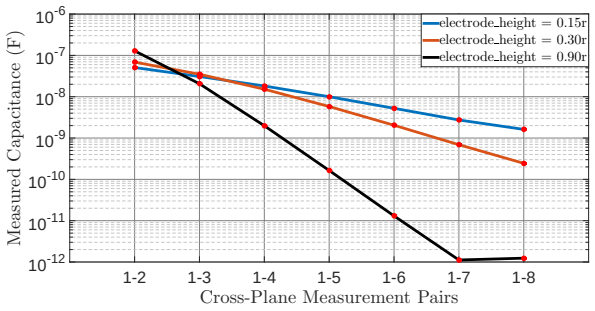

(b)

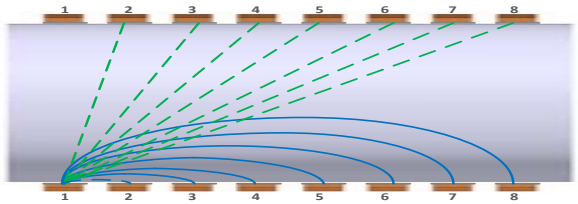

(c)

Fig. 1. (a) Cross-plane mutual capacitance measurements between electrode in layer 1 and other layers vertically aligned to it (solid blue lines in bottom figure). (b) Cross-plane mutual capacitance measurements between electrodes in layer 1 and other layers that are on the opposite side of the sensor (green dashed lines in bottom figure). (c) Electrode pairs for the results in (a) (solid lines) and (b) (dashed lines).

of the image reconstruction problem. As a result, there should be an optimal number of cross-plane measurements. Li and Holland [24] suggested that to obtain volumetric images one does not necessarily need measurements from electrode pairs that are separated by one or more sensor planes. While this is certainly true, the final quality of the volumetric images should nevertheless depend on the number of cross-layer measurements. In this work, we investigate in detail the optimal number of cross-plane acquisitions to minimize both acquisition times and measurement redundancy while providing increased image resolution. The investigation examines the impact of different numbers of cross-plane acquisitions on (a) the condition number of the sensitivity matrix of the tomography problem, (b) the computational costs of the image reconstruction, and (c) the quality of the reconstructed images. Several simulation and experimental ECVT results are provided to support the conclusions.

II. Electrical Capacitance Volume Tomography

The ECVT forward problem obtains mutual capacitance measurements from electrodes at the RoI boundary given a spatial distribution of the permittivity $\varepsilon(x, y, z)$ within the RoI [25]. The ECVT inverse problem seeks to reconstruct the permittivity distribution given a set of mutual capacitance measurements [26]–[29]. Under a linear Born approximation the forward problem writes as

$$\mathbf{c} = \mathbf{S}\mathbf{g}, \tag{1}$$

where $\mathbf{c}$ is the $M \times 1$ normalized capacitance vector, $\mathbf{S}$ is the $M \times N$ sensitivity (Jacobian) matrix [30], and $\mathbf{g}$ is the $N \times 1$ normalized permittivity vector. In ECVT, mutual capacitance data is extracted by exciting an individual electrode with an AC voltage signal while all other electrodes are grounded and measuring the current at the terminals of all other electrodes. This voltage excitation is then cycled through all the electrodes. If the total number of electrodes is n, there will be a total of $M = n(n-1)/2$ independent mutual capacitance measurements.

In practice, $M \ll N$ and the simplest way to approximate the unknown $\mathbf{g}$ given $\mathbf{c}$ in the inverse problem is by using linear back projection, i.e.

$$\mathbf{g} = \mathbf{S}^T\mathbf{c}. \tag{2}$$

Although a very fast method for qualitative analysis, images obtained by back projection are highly blurred in ECVT. To obtain better images, iterative reconstruction techniques [31]–[33] such as iterative Landweber method (ILM) [34] with regularization strategies are implemented. In its simplest form, ILM can be implemented as

$$\mathbf{g}_{k+1} = \mathbf{g}_k - \alpha_k\mathbf{S}^T(\mathbf{S}\mathbf{g}_k - \mathbf{c}), \tag{3}$$

where α_k is the penalty factor of iteration k. To provide a fair comparison between results based on different measurement acquisitions, all the ECVT image results that follow are based on ILM.

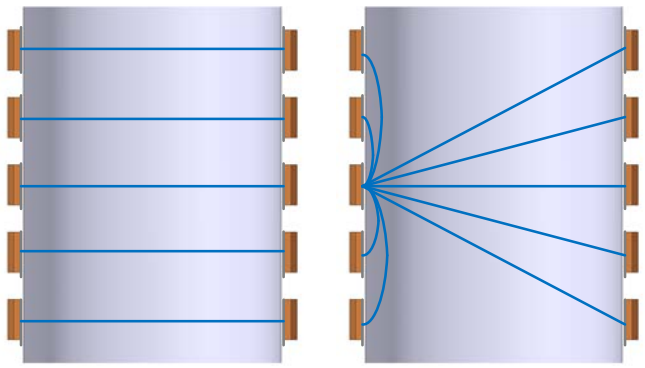

(a) (b)

Fig. 2. (a) Sensing strategy for 3D-ECT imaging, denoted by E_o, (b) sensing strategy for full ECVT imaging, denoted by E_f.

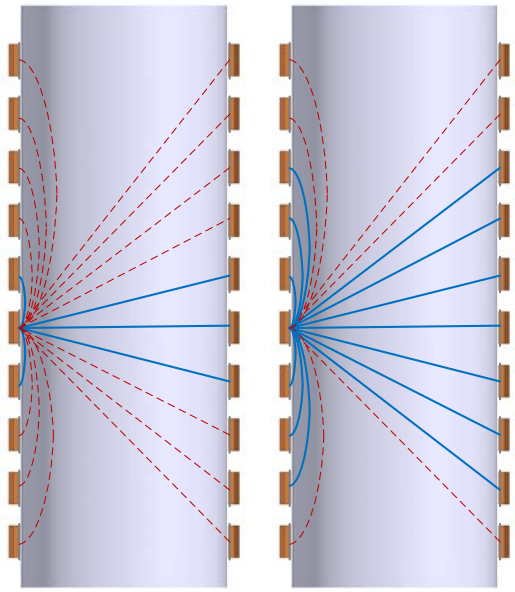

(a) (b)

Fig. 3. (a) Illustration of the E_1 cross-plane sensing strategy for ECVT. (b) illustration of the E_3 cross-plane sensing strategy for ECVT. Given an activated electrode in the sixth layer from top to bottom, the solid blue lines connect the electrode pairs for which mutual capacitance is measured. On the other hand, measurements are not done for the electrode pairs connected by the dashed red lines. This arrangement is repeated for activated electrodes in all other layers.

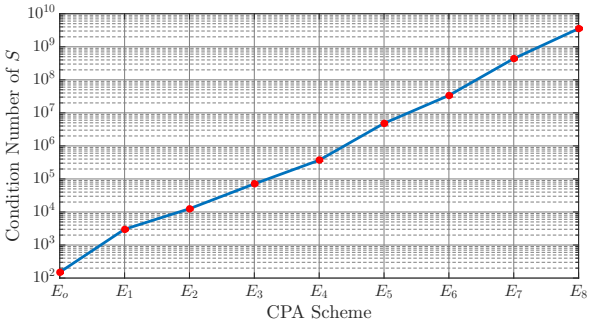

Fig. 4. Condition number of the sensitivity matrix $\mathbf{S}$ obtained using different cross-plane sensing strategies E_n.

III. Cross-Plane Acquisitions (CPA) for ECVT

We refer to a setup where no cross-plane measurements are utilized to obtain volumetric images as 3D-ECT. This is illustrated in Fig. 2a. In contrast, ECVT refers to setups where any number of cross-plane acquisitions (CPAs) are included, as illustrated in Fig. 2b where all four cross-plane acquisitions (two below and two above) are included when exciting an electrode in the middle layer. 3D-ECT acquisition is faster and adequate for predominantly columnar and stratified flows. However, 3D-ECT may not provide accurate axial resolution of more complex multiphase flows such as bubbly flows. To improve on the axial resolution ECVT imaging utilizing cross-plane measurements is desirable. For an ECVT sensor comprising say, about 2 or 3 cross-planes in total, the imaging problem utilizing *all* cross-plane measurements remains quite manageable. As expected however, the imaging problem becomes progressively more challenging for higher number of cross-planes. For example, let us consider a single layer 8 electrode ECT sensor, a 4 layer 8 electrode ECVT sensor and a 10 layer 8 electrode ECVT sensor. The single layer sensor yields 28 independent mutual capacitance measurements, the 4 layer sensor yields 496 such measurements and the 10 layer sensor yields 3160 such measurements, assuming all cross-plane measurements are included. As noted before, the increase on the number of measurements does not come with a proportional increase on the acquired information due to the progressively larger correlation between the additional measurements and the low mutual capacitance values between widely separated cross-planes.

An optimized ECVT acquisition scheme that reduces the cross-plane measurements – effectively constraining the ill-conditioning of the problem – while retaining the quality of the volumetric image reconstruction can be devised to solve the problem. For future reference let us denote the various cross-plane acquisition schemes by E_n, where n is the number of cross-plane measurements below and above the excitation plane. For example, E_0 refer to 3D-ECT (no cross-plane measurements). Fig. 3 shows E_1 and E_3 respectively. We know that for a n number of sensor there will a total of $n(n-1)/2$ measurement. For a $m\times n$ (e.g., m is number sensor layers and n is number of electrode in each layer) ECVT sensor the number of measurements in E_n can be calculated by

$$M = m\frac{n(n-1)}{2} + n^2\sum_{k=1}^{d} m - k, \tag{4}$$

$$M = \frac{n(n-1)}{2}m + \frac{2md - d^2 - d}{2}n^2, \tag{5}$$

where, d is the number of active layers in Cross-Plane acquisition. Substituting $d = m-1$ will result into $mn(mn-1)/2$, which is the total number of independent mesurments for a $m \times n$ ECVT sensor. In addition, E_f refers to the full ECVT acquisition, i.e. where all possible mutual capacitance measurements are included. Fig. 4 shows the condition number of $\mathbf{S}$ matrix of a 10 layer 8 electrode ECVT sensor for various E_n in a reference (air-filled) RoI. The sensor dimensions in this case are the same as in Section IV. It is clear that the condition number of $\mathbf{S}$ matrix increases rapidly as n increases, making the imaging problem more challenging.

The ECVT sensitivity matrix and its condition number are determined by the interrogating field in the RoI. ECVT sensors operate in the quasi-static limit, where the interrogating field in the RoI is a solution of Laplace equation. Because the latter is scale invariant, the behavior of the condition number shown in Fig. 4 remains the same for ECVT sensors of different sizes where all characteristics dimensions (radius, electrode heights, etc.) are scaled by the same factor. The impact of different E_n choices on the quality of the reconstructed images by ECVT sensors is studied in the next section for different types of multiphase flows present in the RoI.

IV. Simulation Results

Fig. 5 depicts the simulation setup. Simulation results are obtained using the Comsol^{TM} finite element solver [35]. The inner and outer diameters of the vessel are 5.35 inches and 5.7 inches respectively. The ECVT sensor surrounding the RoI consists of a total of 80 identical electrodes, with 10 layers and 8 electrodes in each layer. The separation gap between adjacent electrodes is 11.25° along azimuth and 0.56 inches along the axial direction. The height of each individual electrode is 0.84 inch. Two phase vertical flows consisting air and oil as shown in Fig. 5 are considered here for simulation, with relative permittivities set to 1 and 3, respectively. Gaussian noise is added to the simulated data to mimic a measurement acquisition with 60 dB SNR after averaging 10 consecutive signal frames.

Fig. 6 and Fig. 7 shows the reconstructed images of the flow type shown in Fig. 5b and Fig. 5c respectively. The top images in Fig. 6 and Fig. 7 show the qualitative bubble representation using data thresholding and the bottom images show the corresponding quantitative permittivity reconstruction. Fig. 6a and Fig. 7a show the images obtained using E_0 (3D-ECT). It can be observed that 3D-ECT fails to reconstruct the bubbles correctly in both images due to its lack of sufficient axial resolution. However, 3D-ECT can provide good reconstruction for the columnar portion of the flow as seen in this same figure. Fig. 6d and Fig. 7d show the reconstructed images obtained using E_f (full ECVT). This case provides good reconstruction for the bubbles but the columnar portion of the flow in Fig. 7d seems to overpower the bubbly portion in the RoI. This may be caused by the soft-filed nature of the tomography problem and implemented different sensor techniques [36] may improve the results but currently out of the scope of this paper.. Fig. 6b and Fig. 7b show the reconstructed images obtained using E_1 (Fig. 3a). Finally, Fig. 6c and Fig. 7c show the reconstructed images obtained using E_3 (Fig. 3b). It is clear from these results that both E_1 and E_3 provide better volumetric images compared to 3D-ECT and full ECVT, especially in the mixed columnar-bubbly flow case.

For qualitative analysis, the images obtained using E_1 and E_3 provide very similar results, and hence using E_1 would suffice. For quantitative analysis, E_1 may not provide sufficiently accurate results depending on flow scenario, as seen in Table I. For the bubbly flow in Fig. 6, the reconstructed permittivities obtained in the bubble volumes using E_0 and E_1 are 2.47 and 2.72 respectively. For the mixed columnar-bubbly in Fig. 7, E_0 and E_1 provide 2.4 and 2.6 respectively in the bubble volumes. On the other hand, Table I shows that both E_3 and E_f provide permittivity reconstructions much closer to the ground truth in all cases considered here.

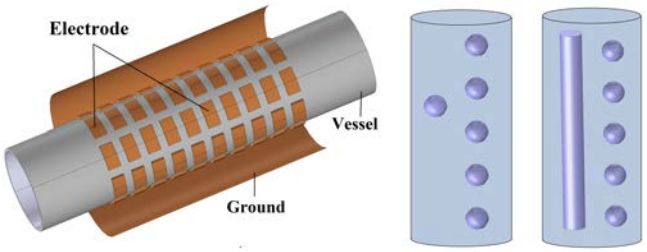

(a) (b) (c)

Fig. 5. (a) Simulation setup for two-phase flow measurements. (b) Bubbly flow. (c) Mixed columnar-bubbly flow.

The results presented in this section clearly indicate that 3D-ECT and full ECVT may fail to provide the best images among the different cross-plane acquisition choices. Both E_1 and E_3 provided good qualitative reconstruction for all cases considered here, but E_1 failed to provide very accurate quantitative permittivity reconstruction in some cases. E_3 provided very accurate permittivity reconstruction in all cases. For qualitative analysis only, E_1 should suffice for most flow types. For quantitative analysis in more general flows of mixed type, an intermediate-order acquisition such as E_3 should be used.

V. Experimental Results

A controlled two-phase flow experiment is conducted to further verify the analysis. A 36-electrode ECVT sensor is used in the experiment, with 6 sensor layers and 6 electrodes in each layer. The height of each electrodes is 0.5 inches and the adjacent electrodes are separated by a 20° gap in azimuth. The vertical gap between successive layers is 0.25 inches. An acrylic cylindrical tube with an inner and outer diameters equal to 4.25 inches and 4.5 inches is used as a vessel for the experiment. Thin hollow plastic balls filled with rice are used here to mimic bubbles in a controlled fashion. The relative permittivity of rice can vary from 2 to 20 depending on the frequency and moisture level [37]. The sensitivity matrix is computed beforehand using a finite element solver given the sensor geometry. Fig. 8 shows the experimental setup used in experiment. In the experiment, two rice-filled balls are kept in place inside the RoI by a thin cotton thread. The measurements are obtained at 500kHz. Each channel has about 60dB SNR level [38].

Fig. 8b shows the picture of the lab controlled flow used in this experiment and Fig. 9 shows the reconstructed images of this controlled experiment. The top images show qualitative volume reconstruction using thresholding and the bottom images show the axial cross-sections of the permittivity images. Fig. 9a, Fig. 9b, Fig. 9c, and Fig. 9d are obtained using E_0, E_1, E_3, and E_f acquisitions, respectively. Reconstructed parmittivities obtained from E_0, E_1, E_3, and E_f are 2.55, 2.87, 2.95, and 2.96 respectively. It is clear from the reconstructed images that E_0 (3D-ECT) does not provide good qualitative and quantitative results. On the other hand, E_1, E_3, and E_f all provide better quantitative and qualitative images. In this particular case, both E_1 and E_3 provide very good reconstruction results so that higher order acquisitions are not needed. See also the results provided in Table I. Reconstruction time presented in Table I indicates that reduced cross plane strategy is a better candidate for real-time monitoring of multiphase flows.

VI. Conclusion

This paper has examined the performance of ECVT for multiphase flow imaging based on different numbers of cross-plane acquisitions. Several simulation and experimental results

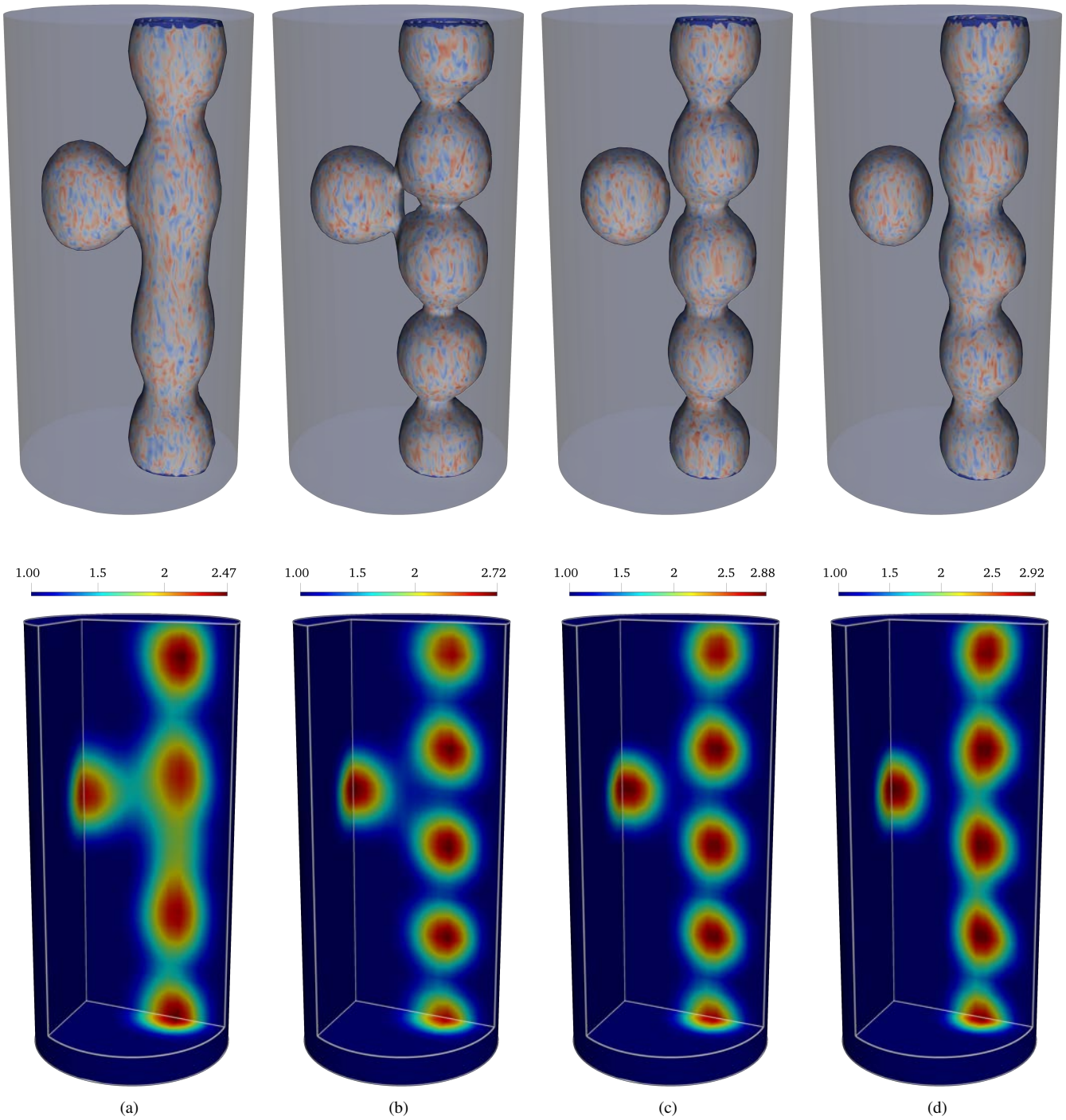

Fig. 6. (a), (b), (c), and (d) shows the reconstructed volumetric images obtained using cross-plane sensing strategy denoted by E_0, E_1, E_3, and E_f respectively. The flow model setup for simulation shown in Fig. 5b. The upper images are a qualitative representation of the volumetric images after thresholding. The bottom images shows the quantitative reconstruction.

TABLE I
E_n ACQUISITION RESULTS

	simulations								experiments			
	Fig. 6				Fig. 7				Fig. 9			
acquisition type	E_0	E_1	E_3	E_f	E_0	E_1	E_3	E_f	E_0	E_1	E_3	E_f
no. of measurements	280	856	1816	3160	280	856	1816	3160	90	270	522	630
no. of ILM iterations	400	400	400	400	400	400	400	400	100	100	100	100
reconstructed ϵ_r in bubble zones	2.47	2.72	2.88	2.92	2.4	2.6	2.8	2.7	2.55	2.87	2.95	2.96
reconstructed ϵ_r in columnar zone	N/A	N/A	N/A	N/A	3	3	3	3	N/A	N/A	N/A	N/A
reconstruction time (sec.)	2.8	7.3	15.8	27.5	2.8	7.8	15.6	28.2	0.1	0.2	0.4	0.7

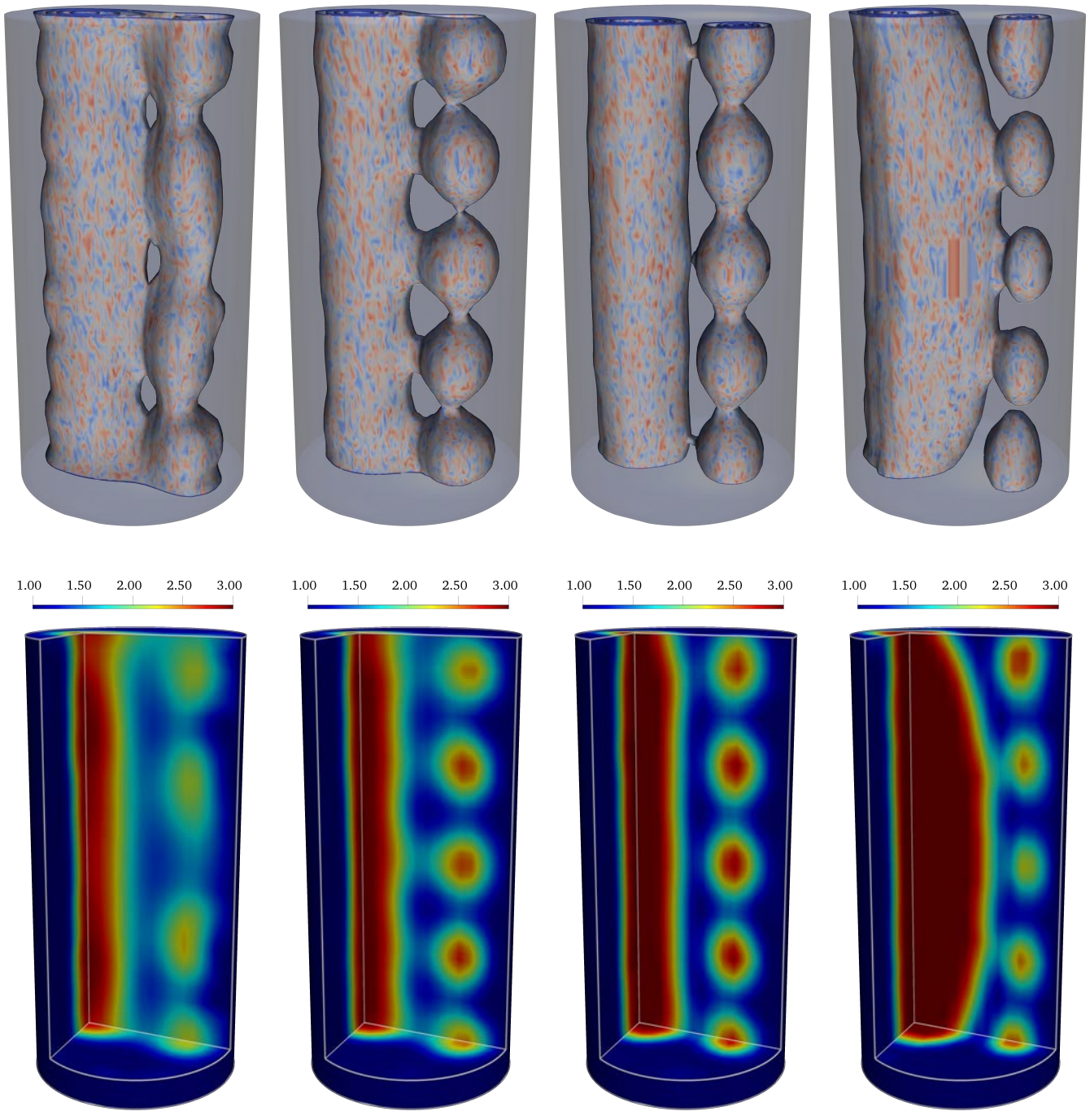

Fig. 7. (a), (b), (c), and (d) show reconstructed volumetric images of a vertical bubbly flow obtained using cross-plane strategies E_0, E_1, E_3, and E_f respectively. The flow model setup for simulation shown in Fig. 5c. The upper images are qualitative representations using thresholding. The bottom images show the actual quantitative reconstruction.

have been presented to show that 3D-ECT, although sufficient for certain types of flows such as columnar flows, has a relatively reduced axial resolution and thus fails to provide accurate quantitative estimation of volumetric images of more complex multiphase flows such as bubbly flows. On the other hand, lower order cross-plane acquisitions were shown to provide a good trade-off between volumetric image quality and measurement acquisition costs. The results show that lower order cross-plane acquisitions are instrumental in constraining the ill-conditioning of the volumetric imaging problem. If, for a given application, quantitative volumetric image estimates are not required, E_1 ECVT acquisition should suffice in most cases and is a good candidate for real-time flow monitoring. On the other hand E_2 and E_3 cross-plane acquisitions enabled retrieval of better quantitative volumetric images still with only moderate costs. In the future, more extensive analysis should be carried out to determine optimal operational bounds of the each type of cross-plane ECVT acquisition versus a wider

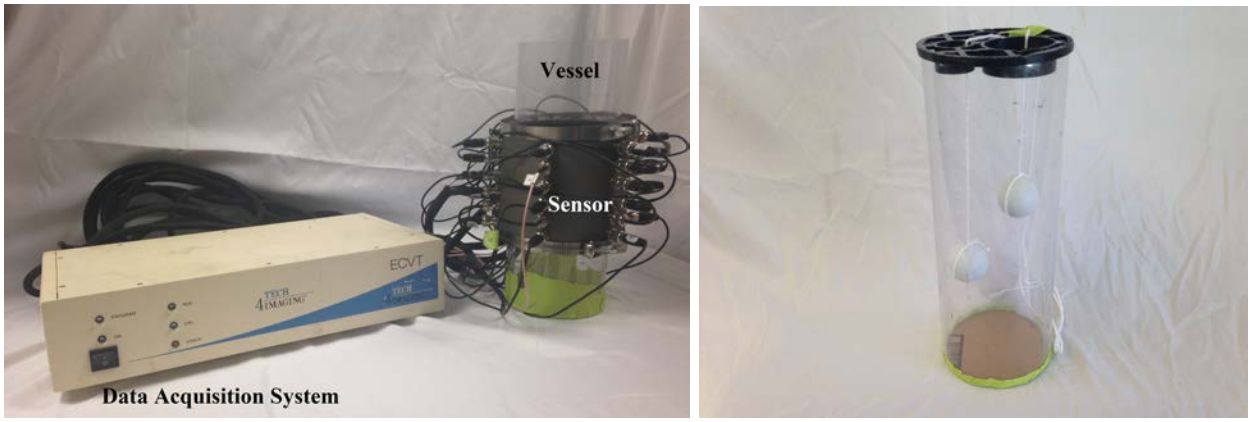

(a) (b)

Fig. 8. (a) Experimental setup to perform ECVT flow measurements. (b) Picture of the flow used in the experiment.

range of possible flow types and sensor geometries.

REFERENCES

[1] L.-S. Fan, *Gas-Liquid-Solid Fluidization Engineering*. Boston: Butterworth-Heinemann, 1989.

[2] S. Huang, C. Xie, J. Salkeld, A. Plaskowski, R. Thorn, R. Williams, A. Hunt, and M. Beck, "Process tomography for identification, design and measurement in industrial systems," *Powder Technology*, vol. 69, no. 1, pp. 85 – 92, 1992.

[3] R. A. Williams and M. S. Beck, *Process Tomography*. Oxford: Butterworth-Heinemann, 1995.

[4] J. M. Weber and J. S. Mei, "Bubbling fluidized bed characterization using electrical capacitance volume tomography (ECVT)," *Powder Technology*, vol. 242, pp. 40 – 50, 2013.

[5] H. Nadeem and T. J. Heindel, "Review of noninvasive methods to characterize granular mixing," *Powder Technology*, vol. 332, pp. 331 – 350, 2018.

[6] N. M. Hasan and B. J. Azzopardi, "Imaging stratifying liquidliquid flow by capacitance tomography," *Flow Measurement and Instrumentation*, vol. 18, no. 5, pp. 241 – 246, 2007.

[7] Y. Li, W. Yang, C. gang Xie, S. Huang, Z. Wu, D. Tsamakis, and C. Lenn, "Gas/oil/water flow measurement by electrical capacitance tomography," *Measurement Science and Technology*, vol. 24, no. 7, p. 074001, 2013.

[8] Y. Li and D. J. Holland, "Optimizing the geometry of three-dimensional electrical capacitance tomography sensors," *IEEE Sensors Journal*, vol. 15, no. 3, pp. 1567–1574, 2015.

[9] K. Perera, C. Pradeep, S. Mylvaganam, and R. W. Time, "Imaging of oil-water flow patterns by electrical capacitance tomography," *Flow Measurement and Instrumentation*, vol. 56, pp. 23 – 34, 2017.

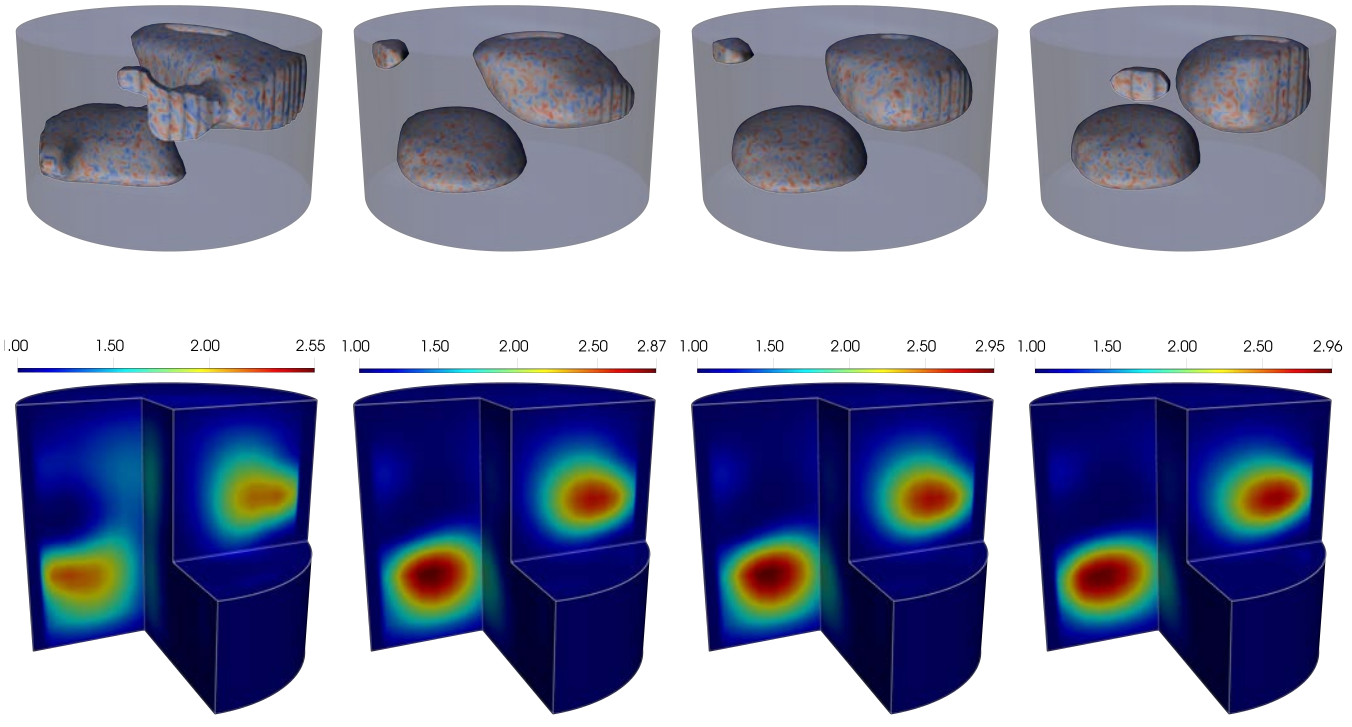

(a) (b) (c) (d)

Fig. 9. (a), (b), (c), and (d) show reconstructed volumetric images of a vertical mixed columnar-bubbly flow obtained using cross-plane strategies E_0, E_1, E_3, and E_f respectively. The upper images are qualitative representations using thresholding and the bottom images show the actual quantitative reconstruction.

[10] Q. Marashdeh, W. Warsito, L. S. Fan, and F. L. Teixeira, "A multimodal tomography system based on ECT sensors," *IEEE Sensors Journal*, vol. 7, no. 3, pp. 426–433, March 2007.
[11] Q. Marashdeh, W. Warsito, , L. S. Fan, and F. L. Teixeira, "Dual imaging modality of granular flow based on ECT sensors," *Granular Matter*, vol. 10, no. 2, pp. 75–80, Jan. 2008.
[12] A. Wang, Q. M. Marashdeh, F. L. Teixeira, and L.-S. Fan, "Electrical capacitance volume tomography: A comparison between 12-and 24-channels sensor systems," *Progress In Electromagnetics Research*, vol. 41, pp. 73–84, 2015.
[13] R. K. Rasel, Q. Marashdeh, and F. L. Teixeira, "Toward electrical capacitance tomography of water-dominated multiphase vertical flows," *IEEE Sensors Journal*, vol. 18, no. 24, pp. 10 041–10 048, 2018.
[14] A. Liao and Q. Zhou, "Application of ECT and relative change ratio of capacitances in probing anomalous objects in water," *Flow Measurement and Instrumentation*, vol. 45, pp. 7–17, 2015.
[15] D. Watzenig and C. Fox, "A review of statistical modelling and inference for electrical capacitance tomography," *Measurement Science and Technology*, vol. 20, no. 5, p. 052002, 2009.
[16] W. Warsito, Q. Marashdeh, and L. S. Fan, "Electrical capacitance volume tomography," *IEEE Sensors Journal*, vol. 7, no. 4, pp. 525–535, April 2007.
[17] Z. Zeeshan, F. Teixeira, and Q. Marashdeh, "Sensitivity map computation in adaptive electrical capacitance volume tomography with multielectrode excitations," *Electronics Letters*, vol. 51, no. 4, pp. 334–336, 2015.
[18] A. Wang, Q. Marashdeh, B. J. Motil, and L.-S. Fan, "Electrical capacitance volume tomography for imaging of pulsating flows in a trickle bed," *Chemical Engineering Science*, vol. 119, pp. 77 – 87, 2014.
[19] Q. Marashdeh and F. L. Teixeira, "Sensitivity matrix calculation for fast 3-D electrical capacitance tomography (ECT) of flow systems," *IEEE Transactions on Magnetics*, vol. 40, no. 2, pp. 1204–1207, March 2004.
[20] S. Chowdhury, Q. M. Marashdeh, and F. L. Teixeira, "Velocity profiling of multiphase flows using capacitive sensor sensitivity gradient," *IEEE Sensors Journal*, vol. 16, no. 23, pp. 8365–8373, 2016.
[21] K. J. Alme and S. Mylvaganam, "Electrical capacitance tomography sensor models, design, simulations, and experimental verification," *IEEE Sensors Journal*, vol. 6, no. 5, pp. 1256–1266, Oct. 2006.
[22] Z. Zeeshan, C. E. Zuccarelli, D. O. Acero, Q. M. Marashdeh, and F. L. Teixeira, "Enhancing resolution of electrical capacitive sensors for multiphase flows by fine-stepped electronic scanning of synthetic electrodes," *IEEE Transactions on Instrumentation and Measurement*, vol. 68, no. 2, pp. 462–473, Feb 2019.
[23] C. Gunes, D. O. Acero, Q. M. Marashdeh, and F. L. Teixeira, "Acceleration of electrical capacitance volume tomography imaging by Fourier-based sparse representations," *IEEE Sensors Journal*, vol. 18, no. 23, pp. 9649–9659, Dec 2018.
[24] Y. Li and D. J. Holland, "Fast and robust 3D electrical capacitance tomography," *Measurement Science and Technology*, vol. 24, no. 10, p. 105406, 2013.
[25] Q. M. Marashdeh, F. L. Teixeira, and L.-S. Fan, "Electrical capacitance tomography," in *Industrial Tomography*, M. Wang, Ed. Woodhead/Elsevier, 2015, pp. 3–21.
[26] K. J. Alme and S. Mylvaganam, "Electrical capacitance tomography–sensor models, design, simulations, and experimental verification," *IEEE Sensors Journal*, vol. 6, no. 5, pp. 1256–1266, Oct. 2006.
[27] Y. S. Kim, S. H. Lee, U. Z. Ijaz, K. Y. Kim, and B. Y. Choi, "Sensitivity map generation in electrical capacitance tomography using mixed normalization models," *Measurement Science and Technology*, vol. 18, no. 7, p. 2092, 2007.
[28] Z. Guo, F. Shao, and D. Lv, "Sensitivity matrix construction for electrical capacitance tomography based on the difference model," *Flow Measurement and Instrumentation*, vol. 20, no. 3, pp. 95 – 102, 2009.
[29] S. Chowdhury, Q. M. Marashdeh, and F. L. Teixeira, "Inverse normalization method for cross-sectional imaging and velocimetry of two-phase flows based on electrical capacitance tomography," *IEEE Sensors Letters*, vol. 2, no. 1, pp. 1–4, March 2018.
[30] Q. Guo, S. Meng, D. Wang, Y. Zhao, M. Ye, W. Yang, and Z. Liu, "Investigation of gas–solid bubbling fluidized beds using ECT with a modified tikhonov regularization technique," *AIChE Journal*, vol. 64, no. 1, pp. 29–41, 2018.
[31] H. Wang and W. Yang, "Measurement of fluidised bed dryer by different frequency and different normalisation methods with electrical capacitance tomography," *Powder Technology*, vol. 199, no. 1, pp. 60 – 69, 2010.
[32] Q. Marashdeh, W. Warsito, L.-S. Fan, and F. L. Teixeira, "A nonlinear image reconstruction technique for ECT using a combined neural network approach," *Measurement Science and Technology*, vol. 17, no. 8, p. 2097, July 2006.
[33] W. Q. Yang and L. Peng, "Image reconstruction algorithms for electrical capacitance tomography," *Measurement Science and Technology*, vol. 14, no. 1, p. R1, 2003.
[34] J. D. Jang, S. H. Lee, K. Y. Kim, and B. Y. Choi, "Modified iterative Landweber method in electrical capacitance tomography," *Measurement Science and Technology*, vol. 17, no. 7, p. 1909, 2006.
[35] *COMSOL™ Multiphysics Reference Guide, version 4.3a*, November 2012.
[36] Z. Cui, W. Zhang, Y. Hu, and H. Wang, "Further development in differential electrical capacitance tomography," *IEEE Sensors Journal*, vol. 18, no. 23, pp. 9781–9791, 2018.
[37] S. H. Noh and S. O. Nelson, "Dielectric properties of rice at frequencies from 50 Hz to 12 GHz," *Transactions of the ASAE*, vol. 32, no. 3, pp. 991–0998, 1989.
[38] R. K. Rasel, C. Zuccarelli, Q. Marashdeh, L. S. Fan, and F. L. Teixeira, "Towards multiphase flow decomposition based on electrical capacitance tomography sensors," *IEEE Sensors Journal*, vol. 17, no. 24, pp. 8027–8036, 2017.

Rafiul K. Rasel received the B.S. degree in electrical engineering (minored in mathematics) and M.S. degree in electrical engineering from the State University of New York at New Paltz, New Paltz, NY, USA in 2013 and 2015, respectively. He is currently a Graduate Research Associate with the ElectroScience Laboratory while pursuing his Ph.D. degree in electrical engineering at The Ohio State University, Columbus, Ohio. His research interests include multiphase flow, capacitive sensing, process tomography, inverse problems, and computational electromagnetics.

Joshua N. Sines received the B.S. degree in Electrical and Computer Engineering from The Ohio State University, Columbus, Ohio, in 2018. He is currently a product engineer for Tech4Imaging, LLC, developing their Electrical Capacitance Volume Tomography (ECVT) technology for use in multiple applications, with a focus on three-phase flow systems.

Qussai Marashdeh received the B.S. degree in electrical engineering from the University of Jordan, Amman, Jordan, in 2001, and both the M.S. and Ph.D. degrees in electrical engineering while affiliated with the Electroscience Laboratory, The Ohio State University, Columbus, in 2003 and 2006, respectively. He also received the M.S in chemical engineering and the M.B.A. from The Ohio State University in 2009 and 2012, respectively.

He is cofounder, President, and CEO of Tech4Imaging LLC, a startup company aimed at advancing capacitance tomography technology and its applications. His research interests include electrical tomography systems, electrostatics, optimization, multiphase flow, and inverse problems.

Fernando L. Teixeira received the Ph.D. degree in electrical engineering from the University of Illinois, Urbana- Champaign in 1999. He was a Postdoctoral Associate with the Massachusetts Institute of Technology during 1999-2000. Since 2000, he has been with The Ohio State University, where he is now a Professor with the Department of Electrical and Computer Engineering and affiliated with the ElectroScience Laboratory. Dr. Teixeira is a recipient of the NSF CAREER Award, the triennial Booker Fellowship from the International Union of Radio Science, and the Outstanding Young Engineer Award from the IEEE Microwave Society (MTT-S). He served as an Associate Editor for the IEEE ANTENNAS AND WIRELESS PROPAGATION LETTERS from 2008 to 2014 and current serves as Associate Editor for *IET Microwaves, Antennas, and Propagation*. His current research interests include electromagnetic sensors, computational electromagnetics, and inverse problems.